This is the accepted manuscript made available via CHORUS. The article has been published as:

Topological Floquet spectrum in three dimensions via a two-photon resonance

Netanel H. Lindner, Doron L. Bergman, Gil Refael, and Victor Galitski

Phys. Rev. B **87**, 235131 — Published 24 June 2013

DOI: 10.1103/PhysRevB.87.235131

Topological Floquet Spectrum in Three Dimensions via a Two-Photon Resonance

Netanel H. Lindner[1,2], Doron L. Bergman[2], Gil Refael[2], Victor Galitski [3,4,5]
1) Institute of Quantum Information, California Institute of Technology, Pasadena, CA 91125, USA.
2) Department of Physics, California Institute of Technology, Pasadena, CA 91125, USA.
3) Center for Nanophysics and Advanced Materials, Department of Physics, University of Maryland, College Park, Maryland 20742-4111, USA
4) Joint Quantum Institute, Department of Physics, University of Maryland, College Park, Maryland 20742, USA. and
5) Kavli Institute for Theoretical Physics, University of California Santa Barbara, CA 93106-4030

Three dimensional (3D) topological insulators display an array of unique properties such as single Dirac-cone surface states and a strong magnetoelectric effect. Here we show how a 3D topological spectrum can be induced in a trivial insulator by a periodic drive, and in particular, using electromagnetic radiation. In contrast to the two-dimensional analog, we show that a two-photon resonance is required to transform an initially unremarkable band structure into a topological Floquet spectrum. We provide an intuitive, geometrical, picture, alongside a numerical solution of a driven lattice model featuring a single surface Dirac mode. Also, we show that the polarization and frequency of the driving electromagnetic field control the details of the surface modes and particularly the Dirac mass. Specific experimental realizations of the 3D Floquet topological insulator are proposed.

I. INTRODUCTION

Three dimensional (3D) topological insulators exhibit a variety of novel electronic properties. Most importantly, their surface states have the spectrum of a *single* massless, chiral two dimensional Dirac fermion. Such surface states were observed recently by angular-resolved photo emission spectroscopy in a variety of new materials, such as Bi_xSb_{1-x} alloys, Bi_2Te_3,and Bi_2Se_3[1–3]. The unusual surface states lead to unique response properties of these materials, e.g., the axion magnetoelectric response[4,5]. Furthermore, these surfaces provide a path for realizing unconventional superconductivity, and in particular to realize and manipulate Majorana Fermions[6], which have important applications for topological quantum computing.

The topological behavior of electrons presents a promising resource, and therefore we must understand all ways to realize it. Here we explore the possibility of dynamically inducing a 3D topological spectrum, surface states included, starting with a trivial (non-topological) bulk insulator. Topological states of time-modulated Hamiltonians were explored in Refs. 7–11. The Floquet spectrum of a periodically driven system was shown to exhibit a variety of topological phases[7]. For instance, graphene is expected to exhibit a quantum Hall effect when subjected to radiation[9,12,13]; a spin-orbit coupled semiconductor heterostructure (such as HgTe/CdTe wells), can be turned topological using microwave-teraHertz radiation[10], and vice versa[14,15].

In this manuscript we demonstrate how to induce a "time reversal invariant" 3D topological spectrum in trivial insulators using electro-magnetic radiation. Roughly speaking, a topologically trivial band structure can be turned topological by mixing the valence and conduction bands by radiative transitions[10]. In 3D, the radiation must be carefully tailored to produce a non-vanishing band mixing matrix element in a closed 2D surface in momentum space, and must obey additional topological and symmetry constraints. Nevertheless, the polarization and frequency of the driving electromagnetic field enable a detailed engineering of the surface states, including the possibility of opening and tuning a gap in the surface Dirac cone.

The paper is organized as follows: In Sec. II, we review a 3D lattice model for a time reversal symmetric, spin orbit coupled insulator which exhibits a transition between a trivial and a topological phase. This model will be used in Sec. III to demonstrate how a topological Floquet spectrum can be induced starting from the trivial phase, using time periodic perturbations. In Sec. IV we describe how to realize this effect using oscillating electromagnetic fields. In Sec. V we discuss several aspects regarding the applications of these ideas to solid state systems, including candidate systems.

II. TOPOLOGICAL TRANSITIONS IN A 3D LATTICE MODEL

In the following, we use a simple generic band structure to develop our ideas. Consider an effective low-energy model near the Γ ($\mathbf{k}=0$) point[3]. The four states near the Fermi energy at the Γ point are labeled using two quantum numbers, corresponding to spin $\sigma =\uparrow,\downarrow$ and parity $\tau = +,-$. Time reversal symmetry (TRS) is represented by $\mathcal{T} = i\sigma_y \otimes I\mathcal{K}$, where $\mathcal{K}$ indicates complex conjugation. Inversion symmetry is represented by $\mathcal{I} = I \otimes \tau_z$. Consider the Hamiltonian

$$H(\mathbf{k}) = \vec{D}(\mathbf{k}) \cdot \vec{\gamma} \tag{1}$$

where $\vec{\gamma} = (\gamma_1, \gamma_2, \gamma_3; \gamma_5)$ are four Dirac matrices, represented by $\gamma_i = \sigma_i \otimes \tau_x$ with $i = 1, 2, 3$, and $\gamma_5 = I \otimes \tau_z$. The remaining dirac matrices are defined as $\gamma_4 = I \otimes \tau_y$

and $\gamma_{ij} = \frac{1}{2i}[\gamma_i, \gamma_j]$. In Eq. (1) and below, we denote 3-dimensional (space coordinate) vectors, such as the momentum, $\mathbf{k}$, in bold symbols, while the 4-dimensional vectors are denoted with a vector symbol $\vec{D}$, and $\hat{D}$ for unit vectors. Writing $\vec{D}(\mathbf{k}) = (\mathbf{d}(\mathbf{k}); D_5(\mathbf{k}))$, we note that the Hamiltonian (1) has both time reversal and space-inversion symmetries under the restriction that the vector $\mathbf{d}(\mathbf{k})$ be odd under inversion, while $D_5(\mathbf{k})$ is an even function.

3D Band insulators with TRS ($\mathcal{T}^2 = -1$) admit a $\mathbb{Z}_2$ classification[16–18], distinguishing a topological phase from a trivial one. The model in Eq. (1) can describe both phases, depending on the choice of parameters. Note that although Eq. (1) does not describe the most general 3D Hamiltonian with TRS, this effective model spans a variety of realistic systems and allows a relatively simple visualization of the $\mathbb{Z}_2$ topological invariant that we now focus on.

At each momentum, $\mathbf{k}$, the Hamiltonian (1) is doubly degenerate. Its eigenstates $\psi_{\mathbf{k}}$ of (1) are also the eigenstates of the rank-two projectors $P_{\pm}(\mathbf{k}) = \frac{1}{2}[I \pm \hat{D}(\mathbf{k}) \cdot \vec{\gamma}]$ onto the valence ($-$) and conduction bands ($+$). We can parameterize the unit vector, $\hat{D}(\mathbf{k}) = \vec{D}(\mathbf{k})/|\vec{D}(\mathbf{k})|$ (lying on a 3D sphere, S^3), using two polar angles, θ and ξ, and an axial angle, ϕ. We define θ as $\cot(\theta_{\mathbf{k}}) = D_5(\mathbf{k})/|\mathbf{d}(\mathbf{k})|$. The angles ξ, ϕ correspond to the spin direction, by the unit vector $\hat{\mathbf{d}}(\xi_{\mathbf{k}}, \phi_{\mathbf{k}}) = \mathbf{d}(\mathbf{k})/|\mathbf{d}(\mathbf{k})|$. Note that $\hat{\mathbf{d}}(\xi_{\mathbf{k}}, \phi_{\mathbf{k}})$ remains undefined at $\theta = 0, \pi$.

Using the above parametrization, the topological invariant of the Hamiltonian (1) can be calculated by considering the map from the 3D Brillouin zone (BZ), which is a 3D torus, T^3, to S^3. The only topological invariant of this map is an integer which counts the number of times the map wraps the target space S^3, also called the degree of the map. Two Hamiltonians of the form (1), for which the degree of the map differs by 2, can be deformed into each other without closing the gap in the spectrum[19], by adding terms not included in (1). Therefore, the $\mathbb{Z}_2$ classification of the insulator (1) is given by the degree of the map mod 2, with even and odd degrees corresponding to trivial and topological insulators respectively.

Near the Γ point, an expansion to order $\mathbf{k}^2$ yields

$$\vec{D}(\mathbf{k}) = (A\mathbf{k}; M - B\mathbf{k}^2), \tag{2}$$

where spherical symmetry can be assumed for convenience[20]. The topological phase of the Hamiltonian (1),(2) occurs for $M/B > 0$. In this case, the angle, θ, changes from $\theta = 0$ at $\mathbf{k} = 0$ to $\theta = \pi$ at $|\mathbf{k}| \gg \sqrt{M/B}$. For each $0 < \theta < \pi$, the vector $\hat{\mathbf{d}}$ wraps a sphere of 2D unit vectors, S^2, which corresponds to a "latitude" on the target space S^3. Therefore, the target space S^3 of the map is covered once in the topological phase.

Now, when $M/B < 0$, the valence band is characterized by $0 \leq \theta < \pi/2$, while the conduction band corresponds to $\pi/2 > \theta \geq \pi$. Therefore, the degree of the map from the BZ to S^3 is zero, leading to a trivial insulator. We note that terms involving other γ matrices can be added to $H(\mathbf{k})$ in Eq. (1), while keeping TRS. Then, the $\mathbb{Z}_2$ topological invariant cannot be calculated using the above simple considerations. However, as long as the added terms do not cause the gap in the spectrum of $H(\mathbf{k})$ to close, the $\mathbb{Z}_2$ invariant does not change.

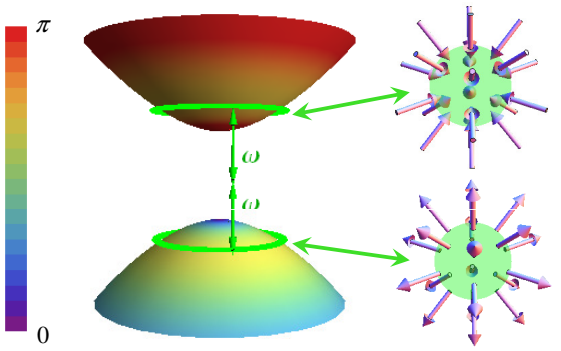

FIG. 1. The two paraboloids represent the dispersion relation $\epsilon_{\pm}(\mathbf{k})$ of the valence and conduction bands for the Hamiltonian (1) in the *trivial* phase, projected on $k_z = 0$. Each energy is doubly degenerate. At each momentum, the projectors $P_{\pm}(\mathbf{k})$ on the eigenstates of (1) can be represented by the spin direction $\mathbf{d}(\xi_{\mathbf{k}}, \phi_{\mathbf{k}})$, and by the angle $\theta_{\mathbf{k}}$ which is encoded by the color scheme. The spin direction on spheres in momentum space, $|\mathbf{k}| = k_0$ is depicted on the right. A two-photon resonance connecting the valence and conduction bands occurs at such a sphere in momentum space, and is represented by the green circles on the parabolas.

III. TOPOLOGICAL FLOQUET SPECTRUM IN THREE DIMENSIONS

Next, let us discuss the non-equilibrium case, where the Hamiltonian Eq. (1) is initially in a trivial phase, and a time-periodic perturbation is added in order to make the system topological. To explore how this may be achieved, we first consider a generic time-dependent perturbation:

$$V(t) = \mathrm{Re}\left(\vec{V} e^{i\omega t}\right) \cdot \vec{\gamma} \tag{3}$$

where $\vec{V}$ is a complex, fixed, four-component vector. Floquet implies that the unitary time-evolution operator of the system, $U(t) = \mathcal{P} \exp\left(-i \int_{t_0}^{t} dt' H(\mathbf{k}, t')\right)$, where $H(\mathbf{k}, t) = H(\mathbf{k}) + V(t)$, can be written as

$$U(t) = W(t) \exp\left[-iH_F(\mathbf{k})t\right], \tag{4}$$

where W is a unitary matrix satisfying $W(t + T) = W(t)$, $T = 2\pi/\omega$ and $H_F(\mathbf{k})$ is a time-independent Floquet operator. The eigenstates of H_F are solutions of $[-i\partial_t + H(\mathbf{k}, t)]\,\Phi(t) = \varepsilon\Phi(t)$ in the space of T-periodic $\Phi(t)$, and ε are the *quasi-energies*. The solutions to the Schrödinger Eq. are of the form $\Psi(t) = e^{-i\varepsilon t}\Phi(t)$.

A topological Floquet spectrum is defined in terms of the topological properties of the time independent Floquet operator[7,10] $H_F(\mathbf{k})$. These can be studied using the available tools for classifying equilibrium Hamiltonians for free fermions[16,17].

To induce a topological Floquet operator $H_F(\mathbf{k})$ in a non-topological parent system, an appropriate choice of $V(t)$ must be made. First, the Floquet operator $H_F(\mathbf{k})$ should be invariant under an effective TRS[21]. This would follow when

$$\mathcal{T}H(\mathbf{k},t)\mathcal{T}^{-1} = H(-\mathbf{k},-t+\tau), \qquad \mathcal{T}^2 = -1 \tag{5}$$

holds for some fixed τ (which can be redefined by choosing the origin of time).[7,10]. The TRS constraint in Eq. (5) is satisfied if $\arg(V_{1,2,3}) = \arg(V_5) + \pi$.

The most dominant effect of the time dependent perturbation $V(t)$ will be to cycle transitions between two states at a given momentum $\mathbf{k}$ that are at, or close to resonance with the frequency ω. These effects are most conveniently studied by using a rotating frame, in which the lower band is shifted up by ω. This is achieved by applying the unitary transformation $\Pi(\mathbf{k},t) = P_+(\mathbf{k}) + P_-(\mathbf{k})e^{-i\omega t}$ (here $P_\pm(\mathbf{k})$ are the projectors defined above) to the (interaction picture) Hamiltonian, which yields:

$$\begin{aligned} H_I(\mathbf{k},t) = \epsilon_+(\mathbf{k})P_+(\mathbf{k}) + [\epsilon_-(\mathbf{k})+\omega]\,P_-(\mathbf{k}) \\ + \Pi(\mathbf{k},t)V(t)\Pi^\dagger(\mathbf{k},t), \end{aligned} \tag{6}$$

where $\epsilon_\pm(\mathbf{k}) = \pm|\vec{D}(\mathbf{k})|$ are the band dispersion relations of $H(\mathbf{k})$. Note that $H_I(\mathbf{k},t)$ and $H(\mathbf{k},t)$ have identical Floquet spectrum.

We now study the spectrum of Eq. (6). Ignoring the last term, when ω overcomes the band gap ($\omega > 2M$), the two bands intersect on a two-sphere in the BZ, $|\mathbf{k}| = k_0$, which we will denote $\mathcal{S}$ (Fig 1). Away from $\mathcal{S}$, the driving term (third term in Eq. (6)) is negligible[22] and the quasi-energy states are roughly eigenstates of $P_\pm(\mathbf{k})$. At $\mathcal{S}$, however, the driving term may induce a new gap in the quasi-energy spectrum. Most crucially, for small momenta, H_I is band inverted compared to the original Hamiltonian. Define the projectors $P^I_\pm(\mathbf{k})$ onto the quasi-energy bands of H_I; $P^I_-(\mathbf{k})$ smoothly interpolates between $P_+(\mathbf{k})$ near the Γ point, and $P_-(\mathbf{k})$ at $|\mathbf{k}| \gg k_0$ (and vice versa for $P^I_+(\mathbf{k})$).

To determine the topological properties of $P^I_\pm(\mathbf{k})$ (and therefore of $H_I(\mathbf{k},t)$) we need to study the form of $P^I_\pm(\mathbf{k})$ near the resonance sphere. For values of $\mathbf{k}$ near the resonance sphere, we use the rotating wave approximation (RWA), and consider only the time independent parts of the third term of Eq. (6). This yields

$$V_{\rm RWA} = \tfrac{1}{2}\Big(P_+\check{V}P_- + P_-\check{V}^\dagger P_+\Big), \qquad \check{V} = \vec{V}\cdot\vec{\gamma}. \tag{7}$$

The topological properties of $P^I_\pm(\mathbf{k})$ are intimately related to the transformation properties of $V_{\rm RWA}$ under the group of spatial rotations in 3D. We assume a representation of spatial rotations where γ_4, γ_5 transform trivially, while $(\gamma_1,\gamma_2,\gamma_3)$ transform as a vector. Since to second order in $\mathbf{k}$ the projectors $P_\pm(\mathbf{k})$ are scalars, the transformation properties of $V_{\rm RWA}$ at this order are determined by those of $\check{V}$.

Importantly, a scalar $\check{V}$ leading to a scalar $V_{\rm RWA}$ yields $P^I_\pm(\mathbf{k})$ with a non-trivial topological $\mathbb{Z}_2$ invariant. In contrast, a purely vector $\check{V}$ (and therefore a vector $V_{\rm RWA}$) yields a $P^I_\pm(\mathbf{k})$ which is topologically trivial. To illustrate this, we use the explicit form of $V_{\rm RWA}$,

$$V_{\rm RWA} = \tfrac{1}{2}\Big(\vec{V_\perp}\cdot\vec{\gamma} + D_i{\rm Im}\{V_j\}\gamma_{ij}\Big) \tag{8}$$

where

$$\vec{V_\perp} = {\rm Re}\{\vec{V}\} - ({\rm Re}\{\vec{V}\}\cdot\hat{D})\hat{D}. \tag{9}$$

Consider two illuminating examples: (i) $\check{V} = V_5\gamma_5$ and (ii) $\check{V} = V_1\gamma_1$, with V_1 and V_5 real. This choice allows us, using Eqs. (8),(9) to approximate $P^I_\pm(\mathbf{k}) \approx \frac{1}{2}(1 \pm \hat{n}(\mathbf{k})\cdot\vec{\gamma})$. Therefore, we can deform $P^I_\pm(\mathbf{k})$ such that $P^I_\pm(\mathbf{k}) \to \tilde{P}^I_\pm(\mathbf{k}) = \frac{1}{2}(1\pm\hat{n}(\mathbf{k})\cdot\vec{\gamma})$ while keeping TRS and without closing the Floquet gap. The topological properties of $P^I_\pm(\mathbf{k})$ are determined by the degree of the map from the BZ to S^3 defined by $\hat{n}(\mathbf{k})$.

In case (i), $\check{V}$ is a scalar under spatial rotations, and hence so is $V_{\rm RWA} = \vec{V_\perp}\cdot\vec{\gamma}$. Therefore, the first three components of $\vec{V_\perp}$ must be proportional to $\mathbf{k}$ while the fifth components is a scalar. Indeed, using Eq. (8) we get

$$\vec{V_\perp} = \Big(-\frac{V_5 D_5}{D^2}A\mathbf{k}, V_5 - \frac{V_5 D_5^2}{D^2}\Big) \tag{10}$$

where $D = |\vec{D}(\mathbf{k})|$. On the resonance sphere $\mathcal{S}$, we have $\hat{n}(\mathbf{k},t)\Big|_{\mathcal{S}} = \vec{V_\perp}/|\vec{V_\perp}|$, which maps $\mathcal{S}$ to an S^2 sphere with fixed latitude $\theta(k_0)$ in the target space S^3. Therefore, $\hat{n}(\mathbf{k})$ defines a map from the BZ to S^3, which maps the Γ point to the *south* pole (since $P^I_-(\mathbf{k}) \approx P_+(\mathbf{k})$ around the Γ point); maps S^2 spheres in the BZ to S^2 spheres ("latitudes") on S^3; and maps $|\mathbf{k}| \gg k_0$ towards the *north* pole of S^3 (since $P^I_-(\mathbf{k}) \approx P_-(\mathbf{k})$ for $|\mathbf{k}| \gg k_0$) . It is therefore a map of degree one, which implies a topological spectrum.

In Case (ii), however, $\check{V}$ and $V_{\rm RWA}$ give a vector representation of spatial rotations. Therefore, the first three components of $\vec{V_\perp}$ must either be scalars or belong to a spin-2 representation of spatial rotations, while the fourth and fifth components must belong to a vector representation. Indeed, an explicit calculation gives

$$\vec{V_\perp} = \Big(V_1\hat{\mathbf{x}} - V_1\frac{A^2k_x\mathbf{k}}{D^2}, V_1\frac{Ak_x}{D}\frac{D_5}{D}\Big) \tag{11}$$

Clearly, on $\mathcal{S}$, the vector $\vec{V_\perp}$ does not wrap around an S^2 sphere on S^3, and the resulting map defined by $\hat{n}(\mathbf{k})$ is topologically trivial.

More generally, $V_{\rm RWA}$ will be a superposition of a scalar and vector component. Whether a topological spectrum is obtained depends on the relative magnitude of the two components.

IV. REALIZATION USING ELECTROMAGNETIC FIELDS

These geometrical considerations are crucial for achieving a 3D topological Floquet spectrum using oscillating electromagnetic fields. The electric field operator is a vector under spatial rotations, rendering it inadequate, by the above discussion, for inducing a topological Floquet spectrum. This challenge is overcome, however, by considering multipole tensors of the electric field. More specifically, the trace of the quadrupole tensor E_iE_j is a scalar under rotations. This scalar would appear in the matrix element of a two photon transition connecting the two bands. To employ this scalar, we need a frequency ω which satisfies $M/2 < \omega < M$, such that interband single-photon resonances (due to linear field effects) are excluded, but two-photon transitions, which are second order in $\mathbf{E}$, are allowed. Note that in order to satisfy the TRS constraint, as defined by Eq. (5), the oscillating field must be *linearly* polarized[10]. An ellipticity in the polarization of the driving field leads to interesting effects, which will be discussed later.

Let us now summarize the analysis of the two-photon effects (for complete details see Appendix A). We choose a gauge $\mathbf{E} = \partial_t \mathbf{A}$, $\phi = 0$, whereby the Hamiltonian becomes $H(\mathbf{k},t) = \vec{D}(\mathbf{k}+\mathbf{A}(t))\cdot\vec{\gamma}$. Choosing $\mathbf{A} = \mathcal{A}_0\cos(\omega t)\hat{\mathbf{x}}$, we obtain the Hamiltonian

$$H(\mathbf{k},t) = \vec{D}'(\mathbf{k})\cdot\vec{\gamma} + \vec{V}_1\cdot\vec{\gamma}\cos(\omega t) + \vec{V}_2\cdot\vec{\gamma}\cos(2\omega t), \quad (12)$$

with $\vec{V}_1 = (A\mathcal{A}_0\hat{\mathbf{x}}\,;\, 2B\mathcal{A}_0 k_x)$, $\vec{V}_2 = (\mathbf{0}\,;\,\frac{1}{2}B\mathcal{A}_0^2)$, and $\vec{D}'(\mathbf{k}) = \left(A\mathbf{k}; M - B\mathcal{A}_0^2 - B\mathbf{k}^2\right)$.

Our focus is the effect of 2ω-terms, arising both from $\vec{V}_2$, and from second order processes in $\vec{V}_1$. Both contributions scale, to lowest order in the light intensity, as $\mathcal{A}_0^2/M$. In order to calculate their effect, we perform two consecutive unitary transformations (see Appendix B for an alternative derivation). We first perform a transformation to a frame rotating with frequency ω, of the form leading to Eq. (6). The new Hamiltonian has no new resonances, and we diagonalize its time independent terms, which yields new eigenvalues and projection operators, denoted by $\varepsilon_\pm^{(1)}(\mathbf{k})$ and $P_\pm^{(1)}(\mathbf{k})$ respectively. A second unitary transformation, $\Pi_2(\mathbf{k},t) = P_+^{(1)} + P_-^{(1)}\exp(-i\omega t)$, yields a new interaction-picture Hamiltonian, in which the two bands cross at a surface $\mathcal{S}$ (topologically, a sphere) with $\varepsilon_+^{(1)}(\mathbf{k}) = (\varepsilon_-^{(1)}(\mathbf{k}) + \omega)$. Applying the rotating wave approximation yields on the resonance surface,

$$H_{2,\mathrm{RWA}}|_{\mathcal{S}} = \tfrac{1}{2}\vec{V}_\perp^{(1)}\cdot\vec{\gamma}. \quad (13)$$

The vector $\vec{V}_\perp^{(1)}$ is defined, to lowest order in $\mathcal{A}_0$ and $\mathbf{k}$, as in Eq. (9) with the replacement $\hat{D} \to \hat{D}^{(1)}$ and $\vec{V} \to \vec{V}^{(1)} \equiv \left((\vec{V}_1 - \vec{V}_2)\cdot\hat{D}\right)\hat{D} + \vec{V}_2$. A detailed derivation of the exact form of $\vec{V}_\perp^{(1)}$ is given in Appendix A. The topological properties of $\vec{V}_\perp^{(1)}$, however, can be read off without referring to its specific form: note that $\vec{V}_2\cdot\vec{\gamma}$ is a scalar under spatial rotations, and according to the discussion in Sec. III, will lead to a non-trivial topological properties of $\vec{V}_\perp^{(1)}$. The contributions from $\vec{V}_1$,produce anisotropy in the gap of the Floquet spectrum, without changing its topological properties.

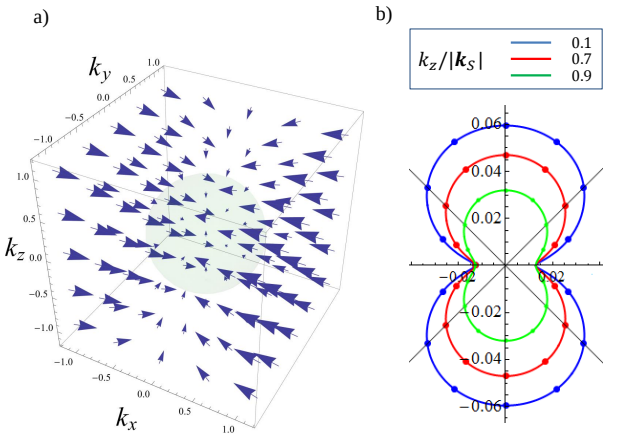

FIG. 2. a) The first three components of the vector field $\vec{V}_\perp^{(1)}(\mathbf{k})$ resulting from a two photon resonance of an electromagnetic field linearly polarized in the x direction. The magnitude of the plotted vector field, on the resonance sphere $\mathcal{S}$ (depicted), gives the gap in the Floquet spectrum. Its direction determines the spin direction of the quasi-energy states on $\mathcal{S}$. The map from $\mathcal{S}$ to the two-sphere S^2, defined by these three components, is of degree one. The resulting gap in the Floquet spectrum is not isotropic, due to the necessary choice of the direction of polarization of the electric field. b) A polar plot showing the gap in the Floquet spectrum. The radial direction gives the magnitude of the gap (in units of M) on the resonance sphere, while the azimuthal coordinate is given by $\tan^{-1}(k_y/k_x)$. Different colors correspond to different values of $|k_z|/|\mathbf{k}_\mathcal{S}|$, where $|\mathbf{k}_\mathcal{S}|$ is the resonance momenta. The parameters chosen are such that $4M = A/|\mathbf{k}_\mathcal{S}| = B/|\mathbf{k}_\mathcal{S}|^2$.

The vector field $\vec{V}_\perp^{(1)}$ for a generic choice of parameters is plotted in Fig. 2. Clearly, it maps $\mathcal{S}$ to a single covering of the unit sphere. The Floquet spectrum is fully gapped at the resonance, with a gap anisotropy that depends on the polarization direction, see Fig. 2b. The smallest gap occurs at resonance momenta $\mathbf{k}_\mathcal{S}$ perpendicular to $\mathbf{E}$, and is given by

$$E_{\mathrm{gap}} = \frac{AB\mathcal{A}_0^2}{2M}|\mathbf{k}_\mathcal{S}| = \eta\frac{\mathcal{W}}{\omega^2}\frac{AB}{2M}|\mathbf{k}_\mathcal{S}|, \quad (14)$$

(in the above, $\mathcal{W}$ is the intensity of the driving field, and $\eta = \frac{e^2\sqrt{\mu/\epsilon}}{\hbar^2}$, where μ and ϵ are the magnetic and dielectric constants in the material)

A striking feature of the topological band structure in 3D is the mid-gap, single Dirac-cone, surface modes[23]. Precisely such surface modes also emerge in the Floquet spectrum due to the driving electric field. We demonstrate this by studying numerically the Floquet problem

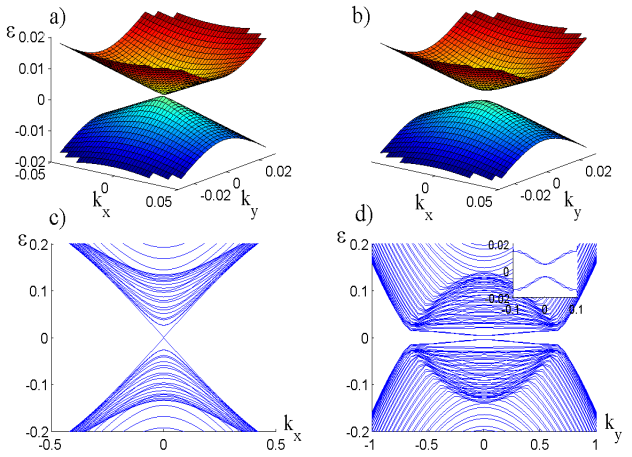

FIG. 3. Quasi-energy spectrum of the Floquet operator for the model (15) in the slab geometry: boundary conditions are periodic in x, y and homogeneous in the z direction. (a) Quasi-energy spectrum inside the bulk gap with a linearly polarized periodic electric field, $\boldsymbol{\varepsilon} = \hat{\mathbf{x}}$, yielding a Dirac cone on the surface. (b) Same as (a) with an elliptically-polarized electric field, $\boldsymbol{\varepsilon} = \hat{\mathbf{x}} + i\delta\hat{\mathbf{y}}$, with $\delta = 0.05$. The ellipticity opens a small gap in the Dirac cone. Note the anisotropy of the Dirac conem due to the polarization of $\hat{\mathbf{x}}$. (c) Quasi-energy spectrum of a linearly polarized field, $\boldsymbol{\varepsilon} = \hat{\mathbf{x}}$, showing bulk bands and edge states as a function of k_x, for $k_y = 0$. Note that at $k_x = k_y = 0$, the smallest Floquet gap occurs at finite k_z. This gap is smaller then the one occuring at $k_y = k_z = 0$ and finite k_x, due to the anistropy arising from the choice of polarization. (d) Spectrum as a function of k_y, for $k_x = 0$, with $\boldsymbol{\varepsilon} = \hat{\mathbf{x}} + i\delta\hat{\mathbf{y}}$. The inset magnifies the gapped Dirac surface spectrum.

of the tight binding Hamiltonian

$$D(\mathbf{k}, t) = \Big(\mathbf{d}(\mathbf{k}); M - 2B(3 - \sum_j \cos(k_j + A_j(t))\Big),$$
$$d_j(\mathbf{k}, t) = A\sin(k_j + A_j(t)), \qquad j = x, y, z, \tag{15}$$

whose low $\mathbf{k}$ expansion corresponds to the model in Eq. (12). We consider a finite slab with homogeneous boundary conditions at $z = 0, L$ and a driving electric field polarized in the $\hat{\mathbf{x}}$ direction. Fig. 3 shows the quasi-energy spectrum inside the quasi-energy gap, which clearly exhibits a Dirac cone.

Broken time reversal symmetry results in a gapped surface mode of 3D topological insulators, which entails unique transport properties[4,5]. Remarkably, a gap of the surface Floquet spectrum can be induced and controlled by choosing an elliptical polarization of the electromagnetic driving field (see Fig 3). Indeed, elliptically-polarized light breaks TRS as it precludes Eq. (5), as shown in Fig 3 b) and d), and allows for control of the edge state spectrum which is unique to the Floquet system.

V. DISCUSSION

The 3D topological Floquet spectrum may be realized in a variety of systems: Cold atoms with synthetic spin orbit couplings[24,25], and even more naturally, semiconductors with direct band-gaps occurring in an odd number of points in the Brillioun zone. By Eq. (14), a narrow bandgap and the use of low- frequency drive are advantageous for achieving a sizeable gap in the Floquet spectrum. Candidate materials are rhombohedral Sb_2Se_3[3], $GeSb_2Te_4$[26], and the gap-tunable Heusler compounds[27,28] with applied strain, and $TlBiSe_x2S_{2-x}$ alloys[29], where a gap of $\sim 10K$ can be achieved using microwave fields of intensity $\leq 1\frac{\mathrm{W}}{\mathrm{mm}^2}$.

As opposed to the its 2D counterpart[10], the surface modes emerging in the 3D driven system, allow direct probing of the driven topological state using a multitude of all-optical means. These include photoemission spectroscopy[30,31]; the measurements of the Kerr and Faraday effect[32], which can detect a gapped Floquet surface spectrum (whereas in the material these effects should be negligible absent the driving); measurement of induced photocurrents[33], and photoluminiscence[34].

In a solid-state realization of our proposal, the electronic distribution in the presence of a periodic drive poses an important question. It was previously studied theoretically and experimentally[34–39], and we intend to address it in future work. According to Ref. 35, coupling to phonons can yield a steady state described by a filled *Floquet* band with an effective temperature (on the order of the lattice temperature). Furthermore, in Ref. 34 the Floquet gap in a semiconductor system is directly observed. These suggest the feasibility of our proposal in solid-state systems.

A finite density of particles and holes in the Floquet bands may attenuate the driving electromagnetic field. By assuming that electrons participating in the band inversion act as free charge carriers[36,37], we estimate a lower bound to the attenuation length, $\xi \approx 1/\sqrt{\omega\mu_e\mu e k_0^3}$, due to carrier density $\sim k_0^3$ and mobility μ_e. By Eq. (14), the localization length λ of the surface modes scales linearly with k_0^{-1}. Therefore, a regime for which $\lambda < \xi$ is attained for $k_0 < \frac{\eta^2}{\mu\mu_e e}\frac{B\mathcal{W}^2}{M\omega^5}$.

ACKNOWLEDGEMENTS

We thank Joseph Avron, Erez Berg, Daniel Podolsky, John Preskill, and Mark Rudner for helpful discussions. VG was supported by NSF CAREER award DMR-0847224. NL was supported by the Gordon and Betty Moore Foundation and NSF through Caltech's Institute of Quantum Information and Matter, and by the National Science Foundation under Grant No. PHY-0803371. DLB was supported by the Sherman Fairchild foundation. GR and VG acknowledge support from DARPA. We are also grateful for the hospitality of the

Aspen Physics Center where part of this work was done. We also acknowledge hospitality of the KITP and the National Science Foundation under Grant No. NSF PHY05-51164.

Appendix A: Topological properties of the two-photon resonance

In this section we study the topological properties of the Floquet operator corresponding to an insulator driven with an electromagnetic field whose frequency allows only for a two photon resonance, $M < \omega < 2M$, where $2M$ is the bandgap of the insulator. The two-photon resonance is a second order process in the electric field. In the chosen gauge, a 2ω-term arises both directly from $\vec{V}_2$, and from a second order process in $\vec{V}_1$. Both terms therefore yield contributions of order $\mathcal{A}_0^2$. In order to consider both terms on an equal footing we shall perform two consecutive time dependent unitary transformations, where each transformation is characterized by the frequency ω. In order to analyze the resulting time dependent Hamiltonian, we shall employ the rotating wave approximation and expand to lowest orders in $\mathbf{k}$ and $\mathcal{A}_0$.

We first introduce some useful notations. We decompose any four dimensional vector $\vec{V}$ into the components parallel and perpendicular to a four dimensional unit vector $\hat{D}$ as

$$\vec{V}_{\perp\hat{D}} = \vec{V} - \left(\vec{V}\cdot\hat{D}\right)\hat{D}, \tag{A1}$$

and

$$\vec{V}_{\parallel\hat{D}} = \left(\vec{V}\cdot\hat{D}\right)\hat{D}. \tag{A2}$$

For notational convenience, we shall relabel $\vec{D}'(\mathbf{k}) \to \vec{D}(\mathbf{k})$, c.f. Eq. (12) in the main text. The first rotating wave transformation is done via the unitary

$$U_1(\mathbf{k},t) = P_+(\mathbf{k}) + P_-(\mathbf{k})e^{-i\omega t}, \tag{A3}$$

which leads to the Hamiltonian in the first rotating frame given by

$$\begin{aligned} H_1 &= U_1(\mathbf{k},t)H(t)U_1^\dagger(\mathbf{k},t) \\ &= \left(\vec{D}(\mathbf{k}) + \tfrac{1}{2}\vec{V}_{1\perp\hat{D}}\right)\cdot\vec{\gamma} + \omega P_-(\mathbf{k}) + \mathcal{V}^{(1)}(t). \end{aligned} \tag{A4}$$

In the above, the time dependent part is given by

$$\begin{aligned} \mathcal{V}^{(1)}(t) = \quad & (\vec{V}_{1\parallel\hat{D}} + \tfrac{1}{2}\vec{V}_{2\perp\hat{D}})\cdot\vec{\gamma}\cos(\omega t) \\ & + \tfrac{1}{2}(\vec{V}_{2\perp\hat{D}})_i\hat{D}_j\gamma_{ij}\sin(\omega t) + \tilde{\mathcal{V}}(t). \end{aligned} \tag{A5}$$

Note that $\mathcal{V}^{(1)}(t)$ contains terms with frequencies ω (the first two term in Eq. (A5)) and $2\omega, 3\omega$ (corresponding to $\tilde{\mathcal{V}}(t)$, the third term above).

It is convenient to define

$$\hat{D}^{(1)}(\mathbf{k}) = \Delta\epsilon(\mathbf{k})\hat{D}(\mathbf{k}) + \tfrac{1}{2}\vec{V}_{1\perp\hat{D}}(\mathbf{k}), \tag{A6}$$

with

$$\Delta\epsilon(\mathbf{k}) = \epsilon(\mathbf{k}) - \tfrac{1}{2}\omega, \qquad \epsilon(\mathbf{k}) = |\bar{D}(\mathbf{k})|, \tag{A7}$$

which enables us to write Eq. (A4) as

$$H_1 = \hat{D}^{(1)}(\mathbf{k})\cdot\vec{\gamma} + \mathcal{V}^{(1)}(t) \tag{A8}$$

The time-independent part of Eq. (A4) can be expressed using eigenvalues $\varepsilon_\pm^{(1)}(\mathbf{k})$ and projection operators $P_\pm^{(1)}(\mathbf{k})$. We now perform a second rotating wave transformation

$$U_2(\mathbf{k},t) = P_+^{(1)}(\mathbf{k}) + P_-^{(1)}(\mathbf{k})\exp(-i\omega t), \tag{A9}$$

which yields the Hamiltonian in the 2^{nd} frame,

$$\begin{aligned} H_2 = {} & \varepsilon_+^{(1)}(\mathbf{k})P_+^{(1)}(\mathbf{k}) + (\varepsilon_-^{(1)}(\mathbf{k}) + \omega)P_-^{(1)}(\mathbf{k}) \\ & + U_2(\mathbf{k},t)\Big((\vec{V}_{1\parallel\hat{D}} + \tfrac{1}{2}\vec{V}_{2\perp\hat{D}})\cdot\vec{\gamma}\Big)U_2^\dagger(\mathbf{k},t)\cos(\omega t) \\ & + U_2(\mathbf{k},t)\Big((\tfrac{1}{2}\vec{V}_{2\perp\hat{D}})_i\hat{D}_j\gamma_{ij}\Big)U_2^\dagger(\mathbf{k},t)\sin(\omega t). \end{aligned} \tag{A10}$$

In the above, we have omitted from H_2 the term $U_2\tilde{\mathcal{V}}(t)U_2^\dagger$ which does not contain any time independent contributions to H_2, and therefore does not contribute to the two photon resonance.

After the second transformations, the two bands cross at a surface $\mathcal{S}$ for which $\varepsilon_+^{(1)}(\mathbf{k}) = (\varepsilon_-^{(1)}(\mathbf{k}) + \omega)$. We now employ the rotating wave approximation. The contribution coming from the second term in Eq. (A10) can be deduced from inspecting Eq. (8) and (9) in the main text. The contribution arising from the third term in Eq. (A10) yields a term of the form $\frac{1}{4i}\hat{D}_i(\vec{V}_{2\perp\hat{D}})_j\hat{D}_k[\gamma_{ij},\gamma_k]$. Some algebra reveals that to lowest order in $\mathcal{A}_0$ and $\mathbf{k}$, the two terms in Eq. (A10) involving $\vec{V}_{2\perp\hat{D}}$ yield the same contribution to the rotating wave approximation.

Therefore, on the surface $\mathcal{S}$ we have,

$$H_{2,\text{RWA}}|_{\mathcal{S}} = \frac{1}{2}\vec{V}^{(1)}_{\perp\hat{D}^{(1)}}\cdot\vec{\gamma} \tag{A11}$$

where the vector $\vec{V}^{(1)}_{\perp\hat{D}^{(1)}}$ is defined as in Eq. (A1) by replacing

$$\hat{D} \to \hat{D}^{(1)}, \qquad \vec{V} \to \vec{V}^{(1)} = \vec{V}_{1\parallel\hat{D}} + \vec{V}_{2\perp\hat{D}}. \tag{A12}$$

In order to achieve a topological Floquet spectrum, the vector field $\vec{V}^{(1)}_{\perp\hat{D}^{(1)}}$ needs to map the resonance surface $\mathcal{S}$ to an S^2 sphere on the three dimensional sphere S^3. In the following we shall show that this is indeed the case.

As a first step, we inspect the contributions to $\vec{V}^{(1)}$, which arise after the first unitary transformation. Keeping only terms only up to second order in $\mathbf{k}$, we find

$$\vec{V}_{1\parallel\hat{D}} = \frac{\mathcal{A}_0(A^2 - 2BM)}{M}k_x\Big(\frac{A}{M}\mathbf{k}, 1\Big),$$

and

$$\vec{V}_{2\perp\hat{D}} = \frac{AB\mathcal{A}_0^2}{2M}\left(\mathbf{k}, -\frac{A}{M}\mathbf{k}^2\right). \tag{A13}$$

The vector field $\vec{V}_{2\perp}$ clearly maps a sphere in the BZ to an S^2 sphere on the target space S^3. This is of course expected from noting that $\vec{V}_2 \cdot \vec{\gamma}$ is a scalar under spatial rotations. However, we are interested in its contribution to the two-photon resonance, *i.e.*, to Eq. (A11).

To this end, we note that $\vec{V}_{2\perp\hat{D}}$ is orthogonal to $\hat{D}$ by construction, and $\hat{D}^{(1)} = \hat{D} + o\Big(\frac{|\vec{V}_{1\perp}|}{\Delta\epsilon}\Big) \approx \hat{D} + o\Big(\frac{|\mathcal{A}_0|}{M}\Big)$. Therefore, the correction to $\vec{V}_{2\perp\hat{D}}$, when it is inserted into the expression for $\vec{V}^{(1)}_{\perp\hat{D}^{(1)}}$, are of higher order in $\mathcal{A}_0$. Explicitly, we have

$$\begin{aligned}\vec{V}_{2\perp\hat{D}} \cdot \hat{D}^{(1)} &= \frac{1}{2|\vec{D}^{(1)}|}\vec{V}_{2\perp}\cdot\vec{V}_1 \\ &= \frac{1}{|\vec{D}^{(1)}|}\frac{AB\mathcal{A}_0^3}{4M}\Big(A + 2\frac{AB}{M}\mathbf{k}^2\Big)k_x \\ &\approx \frac{1}{\Delta\epsilon(\mathbf{k})}\frac{A^2B\mathcal{A}_0^3}{4M}k_x\end{aligned}$$

where we have kept terms only up to order $\mathbf{k}^2$ and $\mathcal{A}_0^3$. Therefore, the final contribution of $\vec{V}_2$ to $\vec{V}^{(1)}_{\perp\hat{D}^{(1)}}$ to this order is

$$\vec{V}_{2\perp\hat{D}^{(1)}} = \vec{V}_{2\perp\hat{D}} - \Big(\frac{A^2B\mathcal{A}_0^3}{4M\Delta\epsilon(\mathbf{k})}k_x\Big)\hat{D} \tag{A14}$$

The second term in the above equation correspond to a correction to the spatial $(1-3)$ parts of $\vec{V}_{2\perp\hat{D}}$, Eq. (A13), of order $\mathbf{k}^2$ and $\mathcal{A}_0^3$. The spatial part of $\vec{V}_{2\perp\hat{D}}$ are originally of order $\mathbf{k}$ and $\mathcal{A}_0^2$. Therefore, to lowest order in $\mathbf{k}$ and $\mathcal{A}_0$, this correction does not alter the topological property of $\vec{V}^{(1)}_{\perp\hat{D}^{(1)}}$, which we shall describe below.

We now calculate the contribution of $\vec{V}_1$ to $\vec{V}^{(1)}_{\perp\hat{D}^{(1)}}$, which will turn out to be of the same order as the contribution of $\vec{V}_2$, c.f. Eq. (A14).

First, we note that

$$\vec{V}_{1\parallel\hat{D}} \cdot \hat{D}^{(1)} = \frac{\Delta\epsilon}{|\vec{D}^{(1)}|}\Big(\vec{V}_1\cdot\hat{D}\Big) \tag{A15}$$

From Eq. (A15), and for $\Delta\epsilon(\mathbf{k}) \gg |\vec{V}_{1\perp\hat{D}}|$, we have

$$\begin{aligned}\big(\vec{V}_{1\parallel\hat{D}}\cdot\hat{D}^{(1)}\big)\hat{D}^{(1)} &= \big(1 - \frac{|\vec{V}_{1\perp\hat{D}}|^2}{8\Delta\epsilon^2}\big)\Big(\vec{V}_1\cdot\hat{D}\Big) \\ &\times \big(1 - \frac{|\vec{V}_{1\perp\hat{D}}|^2}{8\Delta\epsilon^2}\big)\big(\hat{D} + \frac{\vec{V}_{1\perp\hat{D}}}{2\Delta\epsilon}\big)\end{aligned} \tag{A16}$$

Using the definition of $\vec{V}_{1\parallel}$, Eq. (A2), we see that the total contribution of $\vec{V}_1$ to $\vec{V}^{(1)}_{\perp\hat{D}^{(1)}}$, to order $\mathcal{A}_0^2$ is

$$\vec{V}_{1\parallel} - \big(\vec{V}_{1\parallel}\cdot\hat{D}^{(1)}\big)\hat{D}^{(1)} \approx -\frac{\Big(\vec{V}_1\cdot\hat{D}\Big)}{2\Delta\epsilon}\vec{V}_{1\perp} \tag{A17}$$

Therefore, this contribution to $\vec{V}^{(1)}_{\perp\hat{D}^{(1)}}$ is of the *same* order in the driving field as the contribution coming from $\vec{V}_{2\perp\hat{D}}$, Eq. (A13) and its inclusion was necessary for completeness. Note that $\vec{V}_{1\perp} = A\mathcal{A}_0\hat{\mathbf{x}} + o(|\mathbf{k}|)$, and therefore

$$\frac{\Big(\vec{V}_1\cdot\hat{D}\Big)}{2\Delta\epsilon}\vec{V}_{1\perp\hat{D}}\cdot\hat{\mathbf{x}} = \frac{\mathcal{A}_0^2\big(A^2 - 2BM\big)}{2M\Delta\epsilon}Ak_x + o(\mathcal{A}_0^2, |\mathbf{k}|^3) \tag{A18}$$

while the y and z components of Eq. (A17) are of order $\mathcal{A}_0^2$ and $\mathbf{k}^3$. Note that the $\hat{x}_5$ component of Eq. (A17) is of order $\mathcal{A}_0^2$ and $\mathbf{k}^2$. From Eq. (A16), we see that the $\vec{V}_1$ term also contributes terms of order $\mathcal{A}_0^3$ and $\mathbf{k}^2$ to $\vec{V}^{(1)}_{\perp\hat{D}^{(1)}}$. All of the above higher order corrections do not change the topological properties of $\vec{V}^{(1)}_{\perp\hat{D}^{(1)}}$, to lowest order in $\mathcal{A}_0$ and $\mathbf{k}$.

Summing up both contributions to $\vec{V}^{(1)}_{\perp\hat{D}^{(1)}}$, we have, to lowest order in $\mathbf{k}$ and $\mathcal{A}_0$,

$$\begin{aligned}\vec{V}^{(1)}_{\perp\hat{D}^{(1)}}\cdot\hat{\mathbf{x}} &= \Big(\vec{V}_{2\perp\hat{D}} - \frac{\Big(\vec{V}_1\cdot\hat{D}\Big)}{2\Delta\epsilon}\vec{V}_{1\perp}\Big)\cdot\hat{\mathbf{x}} \\ &= \frac{\mathcal{A}_0^2}{2M}\Big(B - (A^2 - 2BM)/\Delta\epsilon\Big)Ak_x,\end{aligned} \tag{A19}$$

while the other two spatial components are given by

$$\vec{V}^{(1)}_{\perp\hat{D}^{(1)}}\cdot\hat{\mathbf{x}}_\alpha = \frac{\mathcal{A}_0^2B}{2M}Ak_\alpha, \qquad \alpha = y, z \tag{A20}$$

From Eqs. (A19,A20), we see that the vector field $\vec{V}^{(1)}_{\perp\hat{D}^{(1)}}$ maps the resonance surface $\mathcal{S}$ to an 2-sphere on the target space S^3. This 2-sphere is not at a constant "latitude", *i.e.* its θ coordinate on S^3 is not constant. Importantly however, this 2-sphere winds around the poles of S^3, *i.e.*, it is an incontractible sphere on the space $S^3 \setminus (N \cup S)$, the space of S^3 with the north and south pole removed.

From the above considerations, we see that $H_2(t)$, given in Eq. (A10) can be characterized by projection operators of the form $P^{(2)}_{\pm}(\mathbf{k}) = \frac{1}{2}(1 \pm \hat{n}_2(\mathbf{k})\cdot\vec{\gamma})$. The unit vector $\hat{n}_2(\mathbf{k})$ defines a map from the BZ to S^3 with the properties: (i) For regions in the BZ near the Γ point, $\hat{n}_2(\mathbf{k}) \approx -\hat{D}(\mathbf{k})$, and therefore it maps 2-spheres in the BZ to 2-spheres on S^3, close to its *south* pole; (ii) Maps the sphere $\mathcal{S}$ in the BZ to an S^2 sphere on S^3 which is incontractible on $S^3 \setminus (N \cup S)$ (as discussed above) ; (iii) For large values of $\mathbf{k}$, $\hat{n}(\mathbf{k}) \approx \hat{D}(\mathbf{k})$, therefore these are mapped to 2-spheres close to the *north* pole of S^3. From continuity of $\hat{n}_2(\mathbf{k})$, it must therefore define a map of degree one. This implies that the Floquet operator corresponding to $H_2(t)$ and $H(t)$, has a non trivial $\mathbb{Z}_2$ topological invariant.

Appendix B: Virtual absorption perturbation theory

The two consecutive RW transformations are very reminiscent of a perturbation expansion. One RW transformation fails to produce a degenracy, and therefore a second transformation is necessary to expose the role of two-photon processes. In this section we will show how indeed such processes can be analyzed as virtual absorption processes, and derive a formula which replaces second-order degenerate perturbation expansions.

The first step involves mapping the time-dependent Floquet problem to a time-independent problem using an auxiliery degree of freedom. Let us introduce an additional Hilbert space which serves as a counter of photons absorbed (for the experts, we note that this auxiliery variable is just a way of keeping track of the Floquet block index). We introduce an infinite lattice for a single particle, which we denote F, with states $|n\rangle_F$; n is essentially counting the number of photons absorbed by the system. The original system has a Hamiltonian which is split to time independent $\mathcal{H}_{sys}$ and time dependent pieces:

$$H(t) = H_{sys} + \hat{O}e^{i\omega t} + \hat{O}^\dagger e^{-i\omega t}, \tag{B1}$$

we now replace the time dependent terms with hopping terms for the register particle F. We also add a diagonal energy term that determines the energy of the F states. The Hilbert space after this mapping is a tensor product state between the F-states and the system's states. The time dependent Hamiltonian is therefore replaced by an operator that acts on the larger Hilbert space,

$$\mathcal{H}_F = \mathcal{H}_{sys} + \sum_n \left(\hat{O} \left|n+1\right\rangle_{F\ F} \left\langle n\right| + \hat{O}^\dagger \left|n\right\rangle_{F\ F} \left\langle n+1\right| \right) + \mathcal{H}_\omega, \tag{B2}$$

with

$$\mathcal{H}_\omega = \sum_n n\omega \left|n\right\rangle_{F\ F} \left\langle n\right|. \tag{B3}$$

and $\mathcal{H}_{sys} = H_{sys} \otimes \mathbb{I}_F$.

To retrieve the original Hamiltonian, Eq. (B1) all that is necessary is to initiate the auxiliary F-states in the zero-momentum state:

$$\left|\psi\right\rangle_F = \frac{1}{N} \sum_n \left|n\right\rangle_F. \tag{B4}$$

with N providing a normalization.

Our first claim is that the time-independent Hamiltonian, Eq. (B2), initiated with $\left|\psi\right\rangle_F$ has the same propagator for the system as the one for the original Hamiltonian, Eq. (B1):

$$U(t) = \mathcal{P}\left[\exp\left[-i\int_0^t dt H(t)\right]\right] =_F \left\langle\psi\right| \exp[i\mathcal{H}_\omega t] \exp\left[-i\mathcal{H}_F t\right] \left|\psi\right\rangle_F. \tag{B5}$$

where $\mathcal{P}$ denotes path ordering. To show this, we first move to the interaction picture in terms of the states F. More precisely we consider:

$$\mathcal{U}(t) = e^{i\mathcal{H}_\omega t} \cdot e^{-i\mathcal{H}_F t}. \tag{B6}$$

We note that

$$\frac{d\mathcal{U}(t)}{dt} = -ie^{i\mathcal{H}_\omega t}(\mathcal{H}_F - \mathcal{H}_\omega)e^{-i\mathcal{H}_\omega t}\mathcal{U}(t). \tag{B7}$$

Since $\mathcal{H}_F - \mathcal{H}_\omega = \mathcal{H}_{sys} + \mathcal{H}_{OF}$, we write:

$$e^{i\mathcal{H}_\omega t}(\mathcal{H}_F - \mathcal{H}_\omega)e^{-i\mathcal{H}_\omega t} = \mathcal{H}_{sys} + \mathcal{H}_{OF}(t) \tag{B8}$$

with:

$$\mathcal{H}_{OF}(t) = e^{i\mathcal{H}_\omega t} \sum_n \left(\hat{O} \left|n+1\right\rangle_{F\ F} \left\langle n\right| + \hat{O}^\dagger \left|n\right\rangle_{F\ F} \left\langle n+1\right| \right) e^{-i\mathcal{H}_\omega t} = \sum_n \left(\hat{O} \left|n+1\right\rangle_F\ _F \left\langle n\right| e^{i\omega t} + \hat{O}^\dagger \left|n\right\rangle_{F\ F} \left\langle n+1\right| e^{-i\omega t} \right). \tag{B9}$$

$\mathcal{U}(t)$ is easily solved to be:

$$\mathcal{U}(t) = \mathcal{P}\left[\exp\left[-i\int_0^t dt\left(\mathcal{H}_{sys} + \mathcal{H}_{OF}(t)\right)\right]\right] \tag{B10}$$

And therefore, the identity (B5), which we are trying to prove, becomes

$$U(t) =_F \langle\psi|\mathcal{U}(t)\,|\psi\rangle_F\,. \tag{B11}$$

Now that we have essentially eliminated $\mathcal{H}_\omega$ from the expression for $U(t)$, the only operators relating to the F-states remaining are the hopping operators $\sum_n |n+1\rangle_F\ {}_F\langle n|$ and $\sum_n |n\rangle_F\ {}_F\langle n+1|$. These operators are simple to handle since $|\psi\rangle_F$ is an eigenstate of both, with eigenvalue 1:

$$\sum_n |n+1\rangle_F\ {}_F\langle n|\,\psi\rangle_F = \sum_n |n\rangle_F\ {}_F\langle n+1|\,\psi\rangle_F = |\psi\rangle_F\,. \tag{B12}$$

Thus we can write:

$$\mathcal{H}_{OF}(t)\,|\psi\rangle_F = |\psi\rangle_F\left(\hat{O}e^{i\omega t} + \hat{O}^\dagger e^{-i\omega t}\right) = |\psi\rangle_F\,H_O(t) \tag{B13}$$

and also:

$$\begin{aligned}\mathcal{U}(t)\,|\psi\rangle_F &= \mathcal{P}\left[\exp\left[-i\int_0^t dt\left(\mathcal{H}_{sys} + \mathcal{H}_{OF}(t)\right)\right]\right]|\psi\rangle_F \\ &= |\psi\rangle_F\,\mathcal{P}\left[\exp\left[-i\int_0^t dt\left(H_{sys} + H_O(t)\right)\right]\right] = |\psi\rangle_F\,U(t)\end{aligned} \tag{B14}$$

which confirms Eq. (B11), and therefore completes the proof of the mapping.

To conclude this section, we note on the correspondence between the formalism presented above and the Floquet theorem

$$U(t) = W(t)\exp\left[-iH_F t\right] \tag{B15}$$

where $W(t+T) = W(t)$ and H_F is an operator acting on the system Hilbert space only, see main text, Eq. (4). The correspondence is given by noting that choosing $W(t=0) = \mathbb{I}$ gives

$$\exp\left[-iH_F t\right] = \langle\psi|_F\exp\left[-i\mathcal{H}_F t\right]|\psi\rangle_F \tag{B16}$$

1. Elimination of single photon processes

The auxiliery F-states formalism allows accounting for a sequence of virtual photon absorptions, by systematically eliminating the F-states associated with intermediate parts of the process. In the case we considered, for instance, there is no resonant single photon process. Therefore, if we start the system and F-state wave function with only an even number of photons, odd-photon F states will only appear with a suppressed amplitude since they have a large energy mismatch with the initial states of the wave function - they must be about an ω away.

Accounting for two-photon processes in our system is thus possible along the lines of ordinary second-order perturbation theory. We start by consdiering the propagator applied to the low-energy subspace, and read-off the effective hamiltonian that emerges after resumming connected diagrams. In our case, the low-energy subspace of the F-states is the superposition of all even states:

$$|\psi_{even}\rangle_F = \frac{1}{N'}\sum_n |2n\rangle_F\,. \tag{B17}$$

The effective two-photon propagator is then given by:

$$U(t) \approx U_2(t) =_F \langle\psi_{even}|\,\mathcal{U}(t)\,|\psi_{even}\rangle_F\,. \tag{B18}$$

Next, we need to expand the interaction Hamiltonian in powers of $\mathcal{H}_{OF}(t)$.

Before carrying out the expansion, let us move to the interaction picture of $\mathcal{H}_{sys}$ as well:

$$e^{i\mathcal{H}_{sys}t}U_2(t) \approx_F \langle\psi_{even}| e^{i\mathcal{H}_{sys}t}\mathcal{U}(t)|\psi_{even}\rangle_F =_F \langle\psi_{even}|\tilde{\mathcal{U}}(t)|\psi_{even}\rangle_F . \tag{B19}$$

with

$$\tilde{\mathcal{U}}(t) = \mathcal{P}\left[\exp\left(-i\int_0^t dt\tilde{H}_{OF}(t)\right)\right]. \tag{B20}$$

We denote

$$\tilde{\mathcal{H}}_{OF}(t) = e^{i(\mathcal{H}_{sys}+\mathcal{H}_\omega)t}\mathcal{H}_{OF}e^{-i(\mathcal{H}_{sys}+\mathcal{H}_\omega)t} = \sum_n \left(\hat{O}(t)|n+1\rangle_F\ {}_F\langle n| e^{i\omega t} + \hat{O}^\dagger(t)|n\rangle_F\ {}_F\langle n+1| e^{-i\omega t}\right). \tag{B21}$$

with $\hat{O}(t) = e^{i\mathcal{H}_{sys}t}\hat{O}e^{-i\mathcal{H}_{sys}t}$.

Now we are ready to expand the interaction Hamiltonian in powers of $\tilde{\mathcal{H}}_{OF}(t)$. Up to second order we encounter the terms:

$$\begin{aligned}\tilde{\mathcal{U}}(t) - 1 = -\int_0^t dt_2\int_0^{t_2} dt_1 \left(\hat{O}(t_2)|n+1\rangle_F e^{i(n+1)\omega t_2} + \hat{O}^\dagger(t_2)|n-1\rangle_F e^{i(n-1)\omega t_2}\right)\left({}_F\langle n|n\rangle_F e^{-in\omega(t_2-t_1)}\right)\\ \left(\hat{O}^\dagger(t_1)_F\langle n+1| e^{-i(n+1)\omega t_1} + \hat{O}(t_1)_F\langle n-1| e^{-i(n+1)\omega t_1}\right).\end{aligned} \tag{B22}$$

Note that we split the compound: $|n\rangle_F\ {}_F\langle m| e^{-i\omega(m-n)t} = |n\rangle_F e^{i\omega nt}\cdot_F\langle m| e^{-i\omega mt}$. The operators $\hat{O}, \hat{O}^\dagger$ could at this point be construed as *first quantized* operators, which change the state of a particle interacting with the radiation field.

Further progress is made by projecting on the initial, intermediate, and final states of the system described by $\mathcal{H}_{sys}$. Let us denote P_σ to be a projector of the system's state on the subspace of energy ϵ_σ. For now, we maintain the generality of the discussion, although eventually, we will restrict ourselves to $H_{sys} = H(\mathbf{k})$ which is a 4×4 Hamiltonian describing two 2d subspaces with energies $\pm\epsilon(\mathbf{k})$; at that point it will be simple to use $\sigma = \pm1$ to indicate the valence vs. conduction subspaces. Armed with this notation we can write:

$$\begin{aligned}\tilde{\mathcal{U}}(t) - 1 = -\sum_{\sigma_1,\sigma_2,\sigma_3}\int_0^t dt_2\int_0^{t_2} dt_1 P_{\sigma_3}\left(\hat{O}(t_2)|n+1\rangle_F e^{i(n+1)\omega t_2} + \hat{O}^\dagger(t_2)|n-1\rangle_F e^{i(n-1)\omega t_2}\right)P_{\sigma_2}e^{-in\omega(t_2-t_1)}\\ \left(\hat{O}^\dagger(t_1)_F\langle n+1| e^{-i\omega(n+1)t_1} + \hat{O}(t_1)_F\langle n-1| e^{-i\omega(n-1)t_1}\right)P_{\sigma_1}\end{aligned} \tag{B23}$$

This allows us to resolve the time dependence of the operators:

$$\begin{aligned}\tilde{\mathcal{U}}(t) - 1 = -\sum_{\sigma_1,\sigma_2,\sigma_3}\int_0^t dt_2\int_0^{t_2} dt_1 P_{\sigma_3}e^{-i(\epsilon_{\sigma_2}-\epsilon_{\sigma_3})t_2}\left(\hat{O}|n+1\rangle_F e^{i(n+1)\omega t_2} + \hat{O}^\dagger|n-1\rangle_F e^{i(n-1)\omega t_2}\right)P_{\sigma_2}\\ \left(\hat{O}_F^\dagger\langle n+1| e^{-i(n+1)\omega t_1} + \hat{O}_F\langle n-1| e^{-i(n-1)\omega t_1}\right)P_{\sigma_1}e^{-i(\epsilon_{\sigma_1}-\epsilon_{\sigma_2})t_1}e^{-in\omega(t_2-t_1)}\end{aligned} \tag{B24}$$

The expressions compactify by defining two indices $\mu_{1,2} = \pm1$, and denoting $\hat{O}^{(+1)} = \hat{O}^\dagger$ and $\hat{O}^{(-1)} = \hat{O}$, and dropping the subscript F,

$$\begin{aligned}\Delta\tilde{\mathcal{U}}(t) - 1 = -\sum_{\sigma_1,\sigma_2,\sigma_3}\sum_{\mu_1,\mu_2=\pm1}\int^t dt_2\int_{-\infty}^{t_2} dt_1 P_{\sigma_3}\hat{O}^{(-\mu_2)}\\ |n+\mu_2\rangle P_{\sigma_2}\hat{O}^{(\mu_1)}\langle n+\mu_1| P_{\sigma_1}e^{-i(\epsilon_{\sigma_1}-\epsilon_{\sigma_2})t_1 - i(n+\mu_1)\omega t_1}e^{-i(\epsilon_{\sigma_2}-\epsilon_{\sigma_3})t_2 + i(n+\mu_2)\omega t_2}e^{-in\omega(t_2-t_1)}\end{aligned} \tag{B25}$$

By moving to average time, $\bar{t} = \frac{t_1+t_2}{2}$ and time difference, $t_- = t_2 - t_1$, as well as integrating over t_- (while assuming that t is large and ignoring boundary terms for t_-, we get:

$$\tilde{\mathcal{U}}(t) - 1 = -\sum_{\sigma_1,\sigma_2,\sigma_3}\sum_{\mu_1,\mu_2=\pm1}\int d\bar{t}P_{\sigma_3}\hat{O}^{(-\mu_2)}|n+\mu_2\rangle P_{\sigma_2}\hat{O}^{(\mu_1)}\langle n+\mu_1| P_{\sigma_1}\frac{ie^{-i\bar{t}\left(\epsilon_{\sigma_1}-\epsilon_{\sigma_3}\right)}e^{-i\bar{t}\omega(\mu_1-\mu_2)}}{\frac{\epsilon_{\sigma_1}+\epsilon_{\sigma_3}}{2} + \omega\frac{\mu_1+\mu_2}{2} - \epsilon_{\sigma_2}} \tag{B26}$$

The time dependence on $\bar{t}$ is simply the interaction-representation time dependence. Therefore, by going back to the Schrödinger representation, we are able to get rid of the remaining time dependence in the expression, and we readily extract the effective second-order contributions to the effective $\mathcal{H}_F$:

$$\mathcal{H}^{eff}_{2-ph} = \sum_{\sigma_1,\sigma_2,\sigma_3}\sum_{\mu_1,\mu_2=\pm1}\sum_n |n+\mu_2\rangle_F\ {}_F\langle n+\mu_1|\frac{P_{\sigma_3}\hat{O}^{(-\mu_2)}P_{\sigma_2}\hat{O}^{(\mu_1)}P_{\sigma_1}}{\frac{\epsilon_{\sigma_1}+\epsilon_{\sigma_3}}{2} + \omega\frac{\mu_1+\mu_2}{2} - \epsilon_{\sigma_2}}, \tag{B27}$$

whereby now

$$\mathcal{H}_F^{eff} = \mathcal{H}_{sys} + \mathcal{H}_{2-ph}^{eff} + \mathcal{H}_\omega \tag{B28}$$

Again we note that $|\psi_{even}\rangle_F$ is an eigenstate with eigenvalue 1 of $\sum_n |n+\mu_2\rangle_{F\ F}\langle n+\mu_1|$ for $\mu_{1,2} = \pm 1$, which allows the mapping back to the original system. As before, the way to go back to the language of the original time dependent problem is to evaluate Eq. (B18), which yields

$$U_2(t) = \mathcal{P}\left[\exp\left[-i\int_0^t dt\left(H_{sys} + H_{2-ph}^{eff}(t)\right)\right]\right], \tag{B29}$$

with

$$H_{2-ph}^{eff}(t) = \sum_{\sigma_1,\,\sigma_2,\,\sigma_3}\ \sum_{\mu_1,\mu_2=\pm 1}\ \sum_n e^{i(\mu_2-\mu_1)\omega t}\frac{P_{\sigma_3}\hat{O}^{(-\mu_2)}P_{\sigma_2}\hat{O}^{(\mu_1)}P_{\sigma_1}}{\frac{\epsilon_{\sigma_1}+\epsilon_{\sigma_3}}{2}+\omega\frac{\mu_1+\mu_2}{2}-\epsilon_{\sigma_2}}, \tag{B30}$$

The form of Eq. (B30) is clearly in accord with degenerate perturbation theory. The reason for the putative degeneracy is the fact that we consider the energy of the F states representing the photons together with the energy of the system. A resonance, therefore, translates to a degeneracy in this language. It is interesting to note that Eq. (B27) generalizes degenerate perturbation theory to the case of near degeneracy. The energy denominator is actually the difference between the average of the initial and final energies, and the intermediate energy.

2. Application to the 3d FTI construction

Applying the formalism above to the 3d FTI construction is quite straightforward. We let $\hat{O} = \hat{O}^\dagger = \frac{1}{2}\hat{V} = \frac{1}{2}\vec{V}\cdot\vec{\gamma}$, and $P_\sigma = \frac{1}{2}\left(1+\sigma\frac{H(\mathbf{k})}{\epsilon_\mathbf{k}}\right)$ with $H(\mathbf{k}) = \bar{D}\cdot\vec{\gamma}$. We separate to two cases: (1) $\sigma_1 = \sigma_3$, $\mu_1 = \mu_2$, and (2)$\sigma_1 = -\sigma_3$, $\mu_1 = -\mu_2 = -\sigma_1$.

a. Case 1 - diagonal elements. The case of diagonal elements can be treated for both the valence and conduction band simultaneously, since terms that do not excite between the bands are time independent, and therefore the f terms factor out. Therefore:

$$\mathcal{H}_{\sigma_1=\sigma_3}^{eff} = |n\rangle_{F\ F}\langle n| \sum_{\sigma_1,\sigma_2=\pm 1,\,\mu=\pm 1}\frac{P_{\sigma_1}\frac{\hat{V}}{2}P_{\sigma_2}\frac{\hat{V}}{2}P_{\sigma_1}}{(\sigma_1-\sigma_2)\epsilon_\mathbf{k}-\mu\omega} \tag{B31}$$

Clearly $\sigma_2 = -\sigma_1$, otherwise the denominator makes the sum vanish. Thus:

$$\mathcal{H}_{\sigma_1=\sigma_3}^{eff} = |n\rangle_{F\ F}\langle n| \sum_{\sigma_1=\pm 1}\frac{P_{\sigma_1}\hat{V}P_{-\sigma_1}\hat{V}P_{\sigma_1}}{4\epsilon_\mathbf{k}^2-\omega^2}\cdot\sigma_1\epsilon_\mathbf{k} \tag{B32}$$

Elementary algebra of the Dirac matrices reduces this expression to:

$$\mathcal{H}_{\sigma_1=\sigma_3}^{eff} = |n\rangle_{F\ F}\langle n| \frac{\left(\vec{V}-\frac{1}{\epsilon_\mathbf{k}^2}\bar{D}\cdot\vec{V}\bar{D}\right)^2}{4\epsilon_\mathbf{k}^2-\omega^2}\frac{1}{2}\bar{D}\cdot\vec{\gamma} \tag{B33}$$

where we also recognize $\vec{V}_{\perp\hat{D}} = \vec{V} - \frac{1}{\epsilon_\mathbf{k}^2}\bar{D}\cdot\vec{V}\bar{D}$. Note that a term corresponding to Eq. (B33) also arises in the treatment involving the two rotating wave transformations. Consider the Hamiltonian $H_2(t)$, Eq. (A10), evaluated at values of $\mathbf{k}$ for which $2\omega = \epsilon(\mathbf{k})$, in the rotating wave approximation. For these $\mathbf{k}$ values, the terms $\varepsilon_+^{(1)}(\mathbf{k})P_+^{(1)}(\mathbf{k}) + (\varepsilon_-^{(1)}(\mathbf{k})+\omega)P_-^{(1)}(\mathbf{k})$ do not vanish, but give, to order $|\vec{V}_1|^2$ a term corresponding to Eq.(B33).

b. Case 2 - interband elements. The interband elements are to some extent more complicated, since we need to consider excitation and relaxation separately. We consider a term connecting the initial state σ_1 with $\sigma_3 = -\sigma_1$. For this process to be viable, we must have $\mu_1 = -\mu_2 = -\sigma_1$. Therefore, the specific term is:

$$\mathcal{H}_{\sigma_1\to-\sigma_1}^{eff} = |n+\mu_2\rangle_{F\ F}\langle n+\mu_1| \sum_{\sigma_2=\pm 1}\frac{P_{-\sigma_1}\frac{\hat{V}}{2}P_{\sigma_2}\frac{\hat{V}}{2}P_{\sigma_1}}{-\sigma\epsilon_\mathbf{k}} \tag{B34}$$

Using the form of P_{σ_2} we can carry out the sum, and obtain:

$$\mathcal{H}^{eff}_{\sigma_1\to-\sigma_1} = |n+\mu_2\rangle_{F\ F}\langle n+\mu_1| \frac{P_{-\sigma_1}\hat{V}H(\mathbf{k})\hat{V}P_{\sigma_1}}{-4\epsilon_k^2} \tag{B35}$$

Once again, elementary manipulations of the Dirac matrices yields:

$$\mathcal{H}^{eff}_{\sigma_1\to-\sigma_1} = \frac{1}{4}|n+\mu_2\rangle_{F\ F}\langle n+\mu_1| \left(-\frac{\vec{V}\cdot\bar{D}}{\epsilon_{\mathbf{k}}^2}\vec{V}_{\perp\hat{D}}\cdot\vec{\gamma} - \frac{\sigma_1}{2}\frac{\vec{V}\cdot\bar{D}}{\epsilon_{\mathbf{k}}^3}\left[\bar{D}\cdot\vec{\gamma},\vec{V}\cdot\vec{\gamma}\right]\right). \tag{B36}$$

This term seems indeed complicated. A simplification occurs, however, when we consider the RWA directly applied with a 2ω energy. The effective Hamiltonian connecting the two bands (that arises from V) is (the RWA eliminates the time dependence, and hence the F's):

$$\mathcal{H}^{eff}_{interband} = \mathcal{H}^{eff}_{1\to-1} + \mathcal{H}^{eff}_{-1\to1} = -\frac{\vec{V}\cdot\hat{D}}{2\epsilon_{\mathbf{k}}}\vec{V}_{\perp\hat{D}}\cdot\vec{\gamma} \tag{B37}$$

This term joins the direct two-photon process that arises from the $\vec{A}^2$ term appearing in D_5 due to the mass curvature. This term also coincides to second order in V, with the corresponding effect on the radiation-induced gap within the two consecutive rotating wave transformations. Note that at resonance $\epsilon_{\mathbf{k}} = 2\Delta\epsilon_{\mathbf{k}}$, and thus Eq. (B37) agrees with Eq. (A19).

[1] D. Hsieh, D. Qian, L. Wray, Y. Xia, Y. S. Hor, R. J. Cava, and M. Z. Hasan, Nature **452**, 970 (2008).
[2] Y. Xia, D. Qian, D. Hsieh, L. Wray, A. Pal, H. Lin, A. Bansil, D. Grauer, Y. S. Hor, R. J. Cava, and M. Z. Hasan, Nat Phys **5**, 398 (2009).
[3] H. Zhang, C.-X. Liu, X.-L. Qi, X. Dai, Z. Fang, and S.-C. Zhang, Nat Phys **5**, 438 (2009).
[4] A. M. Essin, J. E. Moore, and D. Vanderbilt, Physical Review Letters **102**, 146805 (2009).
[5] X.-L. Qi, R. Li, J. Zang, and S.-C. Zhang, Science **323**, 1184 (2009).
[6] L. Fu and C. Kane, Physical Review Letters **100**, 096407 (2008).
[7] T. Kitagawa, E. Berg, M. Rudner, and E. Demler, Physical Review B **82**, 235114 (2010).
[8] T. Kitagawa, M. S. Rudner, E. Berg, and E. Demler, Physical Review A **82**, 033429 (2010).
[9] T. Oka and H. Aoki, Physical Review B **79**, 081406 (2009).
[10] N. H. Lindner, G. Refael, and V. Galitski, Nature Phys. **7**, 490 (2011).
[11] J. P. Dahlhaus, J. M. Edge, J. Tworzydo, and C. W. J. Beenakker, Phys. Rev. B **84**, 115133 (2011).
[12] Z. Gu, H. A. Fertig, D. Arovas, and A. Auerbach, arXiv:1106.0302.
[13] T. Kitagawa, T. Oka, A. Brataas, L. Fu, and E. Demler, arXiv:1104.4636.
[14] B. Dóra, J. Cayssol, F. Simon, and R. Moessner, arXiv:1105.5963.
[15] J.-i. Inoue and A. Tanaka, Phys. Rev. Lett. **105**, 017401 (2010).
[16] A. P. Schnyder, S. Ryu, A. Furusaki, and A. W. W. Ludwig, Physical Review B **78**, 195125 (2008).
[17] A. Kitaev, AIP Conf. Proc. **1134**, 22 (2009).
[18] X.-L. Qi, T. L. Hughes, and S.-C. Zhang, Physical Review B **78**, 195424 (2008).
[19] Z. Wang, X.-L. Qi, and S.-C. Zhang, New Journal of Physics **12**, 065007 (2010).
[20] In the following we consider maps from $\mathbb{R}^3$ to S^3.
[21] In the absence of particle-hole or sublattice symmetries[16–18].
[22] In the following discussion we assume the absence of higher photon resonances, *i.e.*, $\omega > |D(\mathbf{k})|$. Multi photon resonances, do not affect our analysis in this manuscript, and we will consider their interesting effect in future work.
[23] L. Fu, C. L. Kane, and E. J. Mele, Physical Review Letters **98**, 106803 (2007).
[24] T. D. Stanescu, B. Anderson, and V. Galitski, Physical Review A **78**, 023616 (2008).
[25] Y. J. Lin, K. Jimenez-Garcia, and I. B. Spielman, Nature **471**, 83 (2011).
[26] S.-Y. Xu, L. A. Wray, Y. Xia, R. Shankar, A. Petersen, A. Fedorov, H. Lin, A. Bansil, Y. S. Hor, D. Grauer, R. J. Cava, and M. Z. Hasan, arXiv:1007.5111.
[27] S. Chadov, X. Qi, J. Kbler, G. H. Fecher, C. Felser, and S. C. Zhang, Nature Materials **9**, 541 (2010).
[28] H. Lin, L. A. Wray, Y. Xia, S. Xu, S. Jia, R. J. Cava, A. Bansil, and M. Z. Hasan, Nature Materials **9**, 546 (2010).
[29] T. Sato, K. Segawa, K. Kosaka, S. Souma, K. Nakayama, K. Eto, T. Minami, Y. Ando, and T. Takahashi, Nature Physics **7**, 840844 (2011).
[30] D. Hsieh, F. Mahmood, J. W. McIver, D. R. Gardner, Y. S. Lee, and N. Gedik, Physical Review Letters **107**, 077401 (2011).
[31] D. Hsieh, J. W. McIver, D. H. Torchinsky, D. R. Gardner, Y. S. Lee, and N. Gedik, Physical Review Letters **106**, 057401 (2011).
[32] W.-K. Tse and A. H. MacDonald, Physical Review Letters

105, 057401 (2010).
[33] J. W. McIver, D. Hsieh, H. Steinberg, P. Jarillo-Herrero, and N. Gedik, Nature Nanotechnology **7**, 96100 (2012).
[34] Q. T. Vu, H. Haug, O. D. Mcke, T. Tritschler, M. Wegener, G. Khitrova, and H. M. Gibbs, Physical Review Letters **92**, 217403 (2004).
[35] V. M. Galitskii, S. Goreslavskii, and V. F. Elesin, Sov. Phys. JETP **30**, 117 (1970).
[36] L. I. Glazman, Sov. Phys. JETP **53**, 178 (1981).
[37] L. I. Glazman, Sov. Phys. Semi. **17**, 494 (1983).
[38] E. O. Goebel and O. Hildebrand, physica status solidi (b) **88**, 645 (1978).
[39] W. H. Knox, D. S. Chemla, G. Livescu, J. E. Cunningham, and J. E. Henry, Physical Review Letters **61**, 1290 (1988).